ACS OMEGA

http://pubs.acs.org/journal/acsodf

Article

Synthesis of TiO_2−SiO_2−Ag/Fiberglass with Antibacterial Properties and Its Application for Air Cleaning

Aleksandr A. Buzaev, Ekaterina S. Lyutova, Valeriya A. Tkachuk, Lyudmila P. Borilo, and Yu-Wen Chen*

Cite This: *ACS Omega* 2023, 8, 23521−23527

Read Online

ACCESS | Metrics & More | Article Recommendations

ABSTRACT: The TiO_2−SiO_2−Ag/fiberglass with antibacterial properties under UV light irradiation was synthesized. The effects of compositions of TiO_2−SiO_2−Ag/fiberglass, optical, and textural characteristics on the antibacterial activity were studied. The TiO_2−SiO_2−Ag film was coated on the surface of fiberglass carrier filaments. The temperature effect on the formation of the TiO_2−SiO_2−Ag film was established by thermal analysis, and the temperature treatment mode was selected as 300 °C for 30 min, 400 °C for 30 min, 500 °C for 30 min, and 600 °C for 30 min. The influence of silicon oxide and silver additives on the antibacterial properties of TiO_2−SiO_2−Ag films was established. Increasing the treatment temperature of the materials up to 600 °C increased the thermal stability of the titanium dioxide anatase phase, while the values of optical characteristics decreased: the film thickness decreased to 23.92 ± 1.24 nm, the refractive index decreased to 2.154 ± 0.002, the energy of the band gap width decreased to 2.8 ± 0.5, and the light absorption shifted to the visible-light regime, which is important for photocatalytic reactions. The results showed that the use of TiO_2−SiO_2−Ag/fiberglass allows significant decrease in the value of CFU microbial cells to 125 CFU m^{-3}.

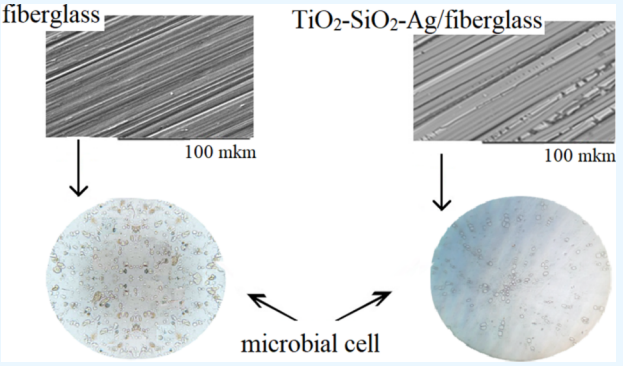

1. INTRODUCTION

The quantitative and species composition of air microflora depend on a number of factors (climatic, meteorological, seasonal, general sanitary condition of the area, etc.). Air quality in the urban environment is an important factor influencing the health of the population. A large variety of pollutants are present in the airspace of cities.[1,2]

Indoor air differs significantly in the composition and number of microorganisms from the atmospheric air. Bacterial contamination of indoor air is always high. Microorganisms dominate in the nasopharynx and skin of humans and animals, including pathogenic species that enter the air by breathing, coughing, sneezing, or talking.[3,4] Microorganisms in sputum and mucus, as well as in epidermal particles, are surrounded by a protein substrate. When such droplets dry out, the protein film has a protective effect; microorganisms persist for a long time, survive and can be transported with air currents over long distances (up to 30 km).[5] However, while the problem of chemical air pollution has been widely studied and reported in the scientific literature, its microbiological condition has received much less attention.[6]

A new effective approach to solve the problem of air purification was the use of photocatalytic oxidation. Currently, air purification units using composite photocatalytic filters are used in the room where it is necessary to clean the air from harmful organic pollutants, bacteria, viruses, and molds.[7] Traditionally, filter-sorbing materials for air purifiers are a carrier with a catalytically active component.[8] Nanoscale inorganic oxides can act as such components in the materials for decontamination and air purification of toxic chemicals.[9,10] Of the most commercial interest is anatase titanium dioxide on the surface of a filter under UV irradiation. Many organic compounds can be oxidized to carbon dioxide and water.[8] The effect of photocatalytic oxidation is based on the titanium dioxide with nanocrystals to generate the electron-excited state and form active oxygen radicals, which oxidize chemical compounds and initiate the reaction to complete mineralization. The process of chemical oxidation takes place at room temperature and atmospheric pressure under UV light irradiation.

In this research, it was proposed to use fiberglass as a carrier for filtering-sorbing material. It is assumed that the filaments that compose fiberglass would allow trapping both gas- and solid-state molecules of air pollutants. This could be an

Received: February 13, 2023
Accepted: June 7, 2023
Published: June 20, 2023

important advantage of using such filter-sorbing materials for air purification devices and solving the problem of filter replacement since the photocatalytic purification method does not accumulate toxic impurities in the filter but decomposes them into carbon dioxide and water.

Composite coating TiO_2−SiO_2−Ag obtained by the sol−gel method was proposed as a photocatalytic active component of the filtering-sorbing material. Using sol−gel technology, we were able to obtain the composite films based on titanium dioxide, silicon dioxide, and silver particles with photosensitivity in the UV light spectrum.[11]

The aim of this work was to develop composite materials with the ability of photocatalytic decomposition of microbiological pollutants under UV light irradiation by introducing nanosized TiO_2 into the structure of fiberglass.

2. EXPERIMENTAL SECTION

2.1. Chemicals. Butyl alcohol (99.9%, Ekos-1, Russia), nitric acid (UralPromDostavka, Russia), tetrabutoxytitanium (TOC, Acros, USA), tetraethoxysilane (TOS, Ekos-1, Russia), silver nitrate (99.9%, LenReactiv, Russia), and fiberglass (JSC Stekloplastik, Russia) were obtained from companies without further purification.

2.2. Synthesis of Materials. The TiO_2−SiO_2−Ag film on the fiberglass surface was obtained by the sol−gel method from a solution of $Ti(OC_4H_9)_4$ (0.1 M), $Si(OC_2H_5)_4$ (0.5 M), $AgNO_3$ (0.06 M) HNO_3 (0.06 M) and H_2O.·In the first step, three components, i.e., butyl alcohol, distilled water, and nitric acid, were mixed to prepare the solution. Then TOC, TOS, and silver nitrate were added to the C_4H_9OH−H_2O−HNO_3 mixture. At the second stage, the above solution was applied to the surface of the fiberglass by impregnation. Then it was dried at 60 °C and step-by-step heat treatment at 300 °C for 30 min, 400 °C for 30 min, 500 °C for 30 min, and 600 °C for 30 min. The heat treatment mode was conditioned by the necessity of complete removal of solvent and crystallization of titanium dioxide in the anatase phase during film formation from solution, as well as by the thermal stability of the selected carrier.

2.3. Characterization. The method of thermal analysis the processes of formation of materials in the course of temperature treatment were studied. The study was carried out on a synchrotron thermal analyzer STA 449C Jupiter (Germany), combined with a mass spectrometer QMS 403 D Aiolos in the temperature range of 30−900 °C in an air atmosphere. The heating rate was 5 °C/min. The sample was loaded in corundum (α-Al_2O_3) crucibles.

The infrared absorption spectra of the films were recorded using a PerkinElmer Spektrum One FTIR Spectrometer in the region of 4000−450 cm^{-1}.

The phase composition of the sample was determined by X-ray diffraction (XRD) on a Rigaku MiniFlex 600 diffractometer (Japan) with a Cu Kα source in the range of reflection angles (2θ) from 10 to 80°. The XRD patterns of the samples were identified using the international data bank PDF-2.

The optical properties of the films were investigated on a LEF-3M ellipsometer with laser radiation (λ = 6328 Å). The ellipsometry method was used to determine the thickness and refractive index of the films. The main advantages of the method are its high sensitivity (up to 10^{-3} nm for effective film thickness). The band gap width of a TiO_2−SiO_2−Ag thin film was determined from the edge of its own absorption band using an EKROS PE-5400UV scanning spectrophotometer in the wavelength range of 190−1000 nm.

The morphology of TiO_2−SiO_2−Ag/fiberglass was studied by scanning electron microscopy (SEM) on a TM-3000 instrument (Hitachi, Japan) at an accelerating voltage of 15 kV (electron gun 5×10^{-2} Pa, sample chamber 30−50 Pa).

The specific surface area, pore volume, and pore size distribution were determined by N_2 adsorption−desorption isotherms using an automatic gas adsorption analyzer TriStarII and a Micromeritics 3Flex device (USA). Before adsorption−desorption measurements, the samples were degassed in vacuum (10^{-2} Torr) for 2 h at 200 °C.

The study of antibacterial properties in relation to the microflora of the air environment was carried out with filtration method in a closed laboratory room with a two-channel aspirator PU-2E with parallel sampling for 30 min during irradiation with UV light with a wavelength of 440 nm. The fiberglass contained the filaments of SiO_2 95 wt %, Al_2O_3 5 wt %, and the resulting TiO_2−SiO_2−Ag/fiberglass material was used as a filter. The bacteria precipitated on the filters were washed with physiological solutions, and the bacterial cultures from these solutions were analyzed on solid nutrient media with the following composition: glucose 5 g/L, peptone 10 g/L, yeast extract 5 g/L, and agar 15 g/L. After seeding microorganisms on nutrient media, the closed Petri dishes were incubated for 3 days at room temperature. Evaluation of antibacterial properties was performed by detecting visible growth zones of incubation strains using an Olympus CX43 optical microscope and counting colony-forming units (CFU) per 1 m^3 of air using the following equation

$$N = (5a \times 10^4)/b \times t \quad (1)$$

where N is the number of CFU m^{-3}; a is the number of CFU grown on the Petri dish; b is the surface area of the Petri dish (cm^2); and t is the exposure time in minutes.

3. RESULTS AND DISCUSSION

3.1. Preparation of Stable Gel Solutions $Ti(OC_4H_9)_4$−$Si(OC_2H_5)_4$−HNO_3−$AgNO_3$−H_2O. In order to obtain thin films, the precursor solutions must satisfy a number of conditions due to certain solution states. The dissolution of precursors requires a time period referred to as the process of "maturation" of the solution or formation of the sol. The duration of this period can be a few minutes or up to several days for different types of substances. At this stage, the transition from a solution to a colloidal solution occurs due to the processes of solvation, hydrolysis, and condensation. Polycondensation is the main chemical process in all stages of sol−gel technology of obtaining materials based on titanium dioxide.

One can identify the existence of three stages: monomer polymerization with particle formation; particle growth; particle binding first into branched chains, then into meshes, eventually spreading to the entire liquid medium and compacting it into a gel.

The transformation of a monomer into a polymer can be considered as a phenomenon equivalent to a phase transformation, and macromolecules should be considered as solid-phase particles, which is true for very dilute solutions. Such solutions are thermodynamically stable systems and can remain in an equilibrium state from several days to several months, depending on the initial substances, solvent, and storage conditions. Films obtained during this stage of maturation of

https://doi.org/10.1021/acsomega.3c00969
ACS Omega 2023, 8, 23521−23527

the film-forming solution, referred to as the time interval of solution stability, are continuous and have reproducible characteristics.

In the next stage, the solution transitions from gel to sol, which corresponds to the aging region of the solution. At this stage, there is a coagulation process, a heterophase system is formed, and the films from such solutions are of poor quality and are not suitable for use.

TOC is highly affected by the hydrolysis and condensation processes. The acidity of the medium and the concentration of water are important parameters in obtaining stable solutions.[12] The viscosity of the film-forming solutions is significantly affected by the nature of the solvent, the concentration of the metal salt, and the second film-forming agent, TOS. The order in which the components are mixed is important: film-forming substances should be introduced into the alcohol solution last. Butanol is more accessible and not as hygroscopic than ethanol. Therefore, it is easier to control the water content, which strongly affects the stability of the solution, in butanol medium.[13,14]

A study of the effect of increasing the concentration of water in the solution (in butanol medium, $Ti(OC_4H_9)_4$ H_2O) showed a significant reduction in its time interval of stability. For a solution with a water concentration of 2 M, an increase in the viscosity of the solution from 3.70 to 4.34 mm^2/s was observed for 60 min, after which a precipitation occurred, indicating the unsuitability of the solution for films. It should be noted that the change in viscosity is non-monotonous, which may indicate that no chemical equilibrium was reached in the solution. For solutions with water concentrations ranging from 0.6 to 1.8 M, the entrainment of viscosity occurred at a slower rate, which slightly extended the stability time interval to 2 h, after which the solution lost its film-forming ability. Decreasing the concentration of water in the solution to 0.2 M led to a significant decrease in the growth rate of viscosity, and after 90 min, the viscosity did not change in the region of 3.9 mm^2/s, which increased the time interval of stability of the solution to 7 days. After 7 days, the viscosity of the solution reached 4.9 mm^2/s, and there was a strong turbidity as a result of precipitation, indicating the absence of film-forming properties of the solution.

Water is the initiator of the hydrolysis process of $Ti(OC_4H_9)_4$. It is known that the resulting hydroxy derivatives of TOC undergo a condensation reaction, with $C_4H_9OH_2^+$ ions serving as the catalyst in butanol medium (2)

$$2H_2O \leftrightarrows H_3O^+ + OH \quad (2)$$

$$2C_4H_9OH \leftrightarrows C_4H_9OH_2^+ + C_4H_9O \quad (3)$$

$$Ti(OC_4H_9)_4 + H_2O \leftrightarrows Ti(OC_4H_9)_3OH + C_4H_9OH \quad (4)$$

$$2Ti(OC_4H_9)_3OH \rightarrow (H_9C_4O)_3Ti\left\langle \begin{matrix} OH \\ OH \end{matrix} \right\rangle Ti(OC_4H_9)3 \quad (5)$$

$$(H_9C_4O)_3Ti\left\langle \begin{matrix} OH \\ OH \end{matrix} \right\rangle Ti(OC_4H_9)_3 \rightarrow (H_9C_4O)_3Ti - O - Ti(OC_4H_9)_3 + H_2O \quad (6)$$

As a result, the molecular weight of the polymers increases, and the viscosity of the solution rapidly increases.

Butanol dissociation processes lead to an increase in the concentration of $C_4H_9OH_2^+$ ions in the solution, as evidenced by the gradual decrease in pH values from 7.71 to 6.9 for the as-prepared solutions.

The addition of nitric acid with a concentration of 0.06 M to the gel increased the viscosity value to 3.8 mm^2/s. This is accompanied with an increase in the time of stabilization of the solution up to 6 h. No change in solution viscosity in the following 40 days was observed. On the 41st day, the viscosity of the solution increased to values of 5.5 mm^2/s and accompanied with gel formation. When using lower concentrations of nitric acid, the stability period of the solution decreased and lead to more rapid gelation. Measurements of the hydrogen index of freshly prepared solutions showed that solutions of $Ti(OC_4H_9)_4$–HNO_3 H_2O with pH in the range of 4.5–4.8 are the most stable. In an acidic environment, the hydrolysis process of TOC occurred at a higher rate, leading to a decrease in the time of transition of the solution to a stable state.

The addition of TOS to the system was carried out as a source of silicon dioxide due to its influence on the parameters of the obtained coatings. The addition of SiO_2 is known to reduce the thickness of composite films and increase the adsorption properties, as well as increase the adhesion to the fiberglass carrier. The time-viscosity change for $Ti(OC_4H_9)_4$–$Si(OC_2H_5)_4$–HNO_3 H_2O solutions was characterized by a slow, smooth growth within 6–7 h and stabilized after 8 h. However, for solutions with concentrations below $Si(OC_2H_5)_4$ 0.3 M, the time interval of stability increased slightly. The solution with a $Si(OC_2H_5)_4$ 0.5 M concentration was stable for 62 days; further increase in the concentration of $Si(OC_2H_5)_4$ in the solution did not affect the duration of the time interval of solution stability.

Introduction of silver nitrate into $Ti(OC_4H_9)_4$–$Si(OC_2H_5)_4$–HNO_3–H_2O solution was due to the necessity to modify the titanium dioxide film from a solution of silver particles. Silver would contact with anatase TiO_2 particles, decreased the energy of interband transitions and increased the photoactivity of the material. Monitoring the viscosity change of the $Ti(OC_4H_9)_4$–$Si(OC_2H_5)_4$–HNO_3 $AgNO_3$–H_2O film-forming solution showed that the addition of silver nitrate in the selected concentration range of 0.1–0.6 M had no effect on the viscosity and stability of the film-forming solutions. The viscosity of $Ti(OC_4H_9)_4$–$Si(OC_2H_5)_4$–HNO_3 $AgNO_3$–H_2O changed similarly to that of $Ti(OC_4H_9)_4$–$Si(OC_2H_5)_4$–HNO_3–H_2O solution and had the same stability time interval of 62 days.

Results of the studies revealed that the solution of $Ti(OC_4H_9)_4$–0.1 M, $Si(OC_2H_5)_4$–0.5 M, $AgNO_3$–0.06 M, HNO_3–0.06 M, and H_2O–0.2 M had a long time interval of stability—62 days, due to the rapid hydrolysis processes of $Ti(OC_4H_9)_4$ and $Si(OC_2H_5)_4$ in the system at a pH value of 4.65, which makes it possible to be a good solution for obtaining thin films with reproducible properties.

3.2. Effect of SiO_2 and Ag Modifying Additives on TiO_2 Properties. For studying the effect of SiO_2 and Ag additives on the formation of titanium dioxide crystalline phases from $Ti(OC_4H_9)_4$–$Si(OC_2H_5)_4$–HNO_3–$AgNO_3$–H_2O solutions, the thin film TiO_2 and TiO_2–SiO_2–Ag materials were obtained. The samples were annealed at different temperatures of 400 °C, 500 °C, and 600 °C, respectively. The results of thermal analysis (Figure 1) indicate

https://doi.org/10.1021/acsomega.3c00969
ACS Omega 2023, 8, 23521−23527

that there were 4 stages of formation for the TiO_2 sample and 5 stages for TiO_2−SiO_2−Ag.

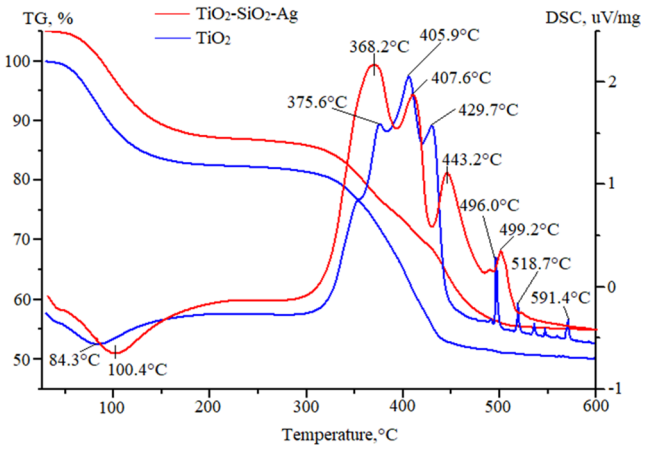

Figure 1. Results of thermal analysis of TiO_2 and TiO_2−SiO_2−Ag samples.

The first stage at temperatures up to 100 °C for TiO_2 and TiO_2−SiO_2−Ag, is characterized by an endothermic process and is due to the removal of physically and chemically bound water and solvent. This is confirmed by the low values of activation energy calculated by the Metzger−Horowitz method of 71.60 and 46.56 kJ for the TiO_2 and TiO_2−SiO_2−Ag systems, respectively.

At temperatures between 300 and 400 °C, the destruction of butoxy groups occurred and titanium dioxide crystallization began for the TiO_2−SiO_2−Ag system, in this temperature range, silver nitrate and ethoxy groups decomposed. The higher values of activation energy from 113 to 415 kJ confirm the chemical nature of the processes taking place.

From 400 to 500 °C, the crystallization of titanium oxide in the anatase modification continued for both systems, while for the TiO_2−SiO_2−Ag system, this process was characterized by a lower value of activation energy. At the same stage, it began the crystallization of silicon oxide and the silver particles for the system TiO_2−SiO_2−Ag. The activation energy for these processes ranged from 165 to 343 kJ. Upon further heating, titanium dioxide was converted from the anatase phase to rutile for the TiO_2 sample, but higher temperatures were needed for the sample containing silicon and silver. This fact is crucial because the anatase phase of titanium dioxide is essential for the synthesis of materials with increasing photoactivity.

Figure 2 shows the IR spectra of TiO_2−SiO_2−Ag samples annealed at 400 °C, 500 °C, and 600 °C, respectively. All IR spectra are characterized by the presence of absorption bands in the 1614−1627 and 3342−3441 cm^{-1} regions, belonging to the strain vibrations of adsorbed and possibly coordination-bound water molecules. As the temperature increased, they moved to the high-frequency region and became less intense, indicating the deepening of the dehydration process of materials. The weak absorption in the region of 2919 cm^{-1} is due to the presence in the composite of degradation products of organic components used in the synthesis.

In the 1027−1032 cm^{-1} region, a small shoulder was observed, which can be attributed to the vibrations of Si−O−Si bonds, the intensity of which increased with increasing temperature. This is due to the separation of signals in the

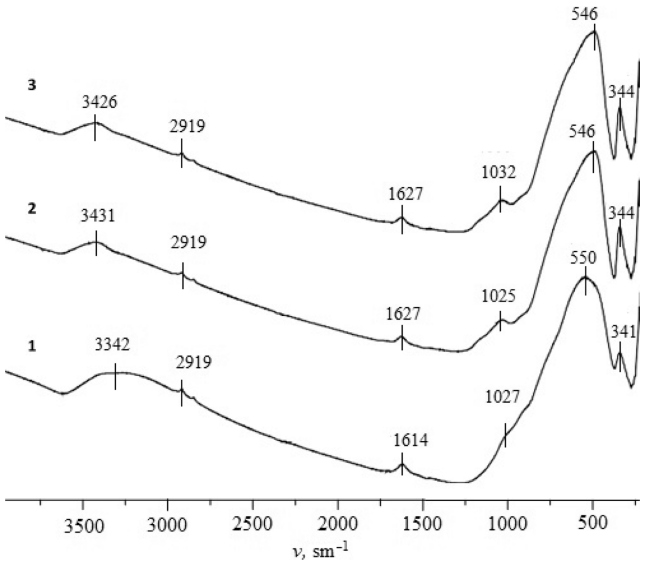

Figure 2. IR spectra of TiO_2−SiO_2−Ag films with different heat treatment temperatures: (1) anneal at 400 °C, (2) 500 °C, and (3) 600 °C.

region of 500−1250 cm^{-1}, which is characteristic of vibrations of Ti−O−Ti, Si−O−Ti, and Si−O−Ti bonds, where the IR spectra show a broad peak. The strongest signals in the spectra are characteristic of the Ti−O−Ti bond vibrations (in the region of 341 and 550 cm^{-1}). Their intensities increased with increasing the temperature of sample processing, which is associated with the process of crystallization of TiO_2, as confirmed by the results of XRD analysis (Figure 3). For comparison, the XRD pattern of a TiO_2 sample without additives calcined in similar conditions (Figure 3a, curves 1−3) shows well-resolved peaks of anatase and rutile phases. The analysis and comparison of the obtained diffractograms were reported in the reference database PDF-2.

Modification of titanium dioxide leads to significant changes in the phase transition temperatures. For TiO_2−SiO_2−Ag, the temperatures of phase transitions of titanium dioxide shifted to the region of higher values. The nature of the diffractogram of TiO_2−SiO_2−Ag calcined at 400 °C indicates the amorphous state of the particles, while the diffractogram of TiO_2 at this temperature showed intense XRD peaks indicating the crystallization of the anatase phase.[15−18] With the increase of heat treatment temperature, the increase of crystallinity of the samples was observed. Heat treatment at 600 °C leads to the formation of the rutile phase for TiO_2 without impurities; therefore, the presence of SiO_2 and Ag in the sample composition retarded the growth of TiO_2 crystals, possibly due to the formation of a solid solution between anatase and silicon dioxide, resulting in increased phase transition temperatures.[19]

The results of micro-X-ray spectral analysis (Figure 4) indicate that the TiO_2−SiO_2−Ag film was represented by the aggregates of loosely packed particles. It can be seen that the sample was a nanostructured system of the fused anatase particles with silicon dioxide interlayers in between. The presence of these silicon dioxide interlayers in the sample reduced the contact between the anatase particles with each other during the sintering process, which inhibited the growth of anatase crystallites and consequently increased the phase transition temperature.

https://doi.org/10.1021/acsomega.3c00969
ACS Omega 2023, 8, 23521−23527

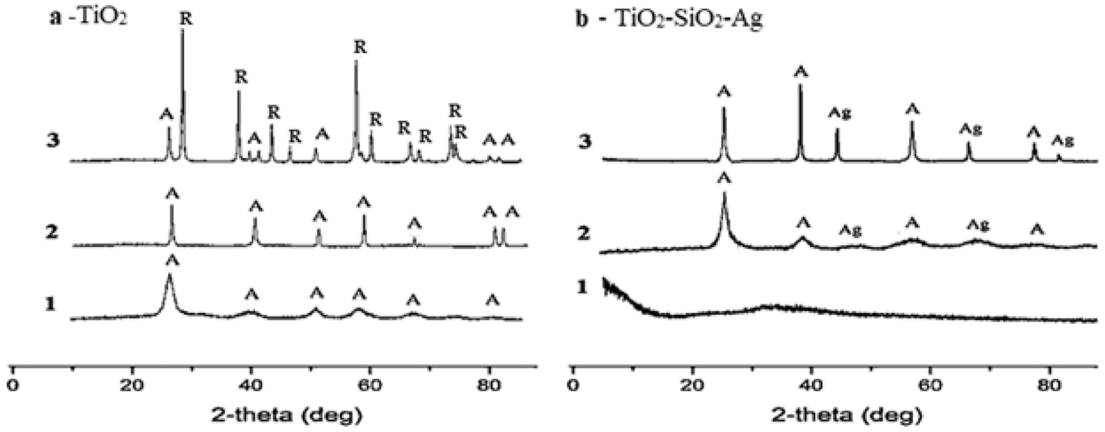

Figure 3. TiO_2 and TiO_2−SiO_2−Ag diffractograms at different heat treatments: 1−400 °C; 2−500 °C; 3−600 °C (A: anatase, R: rutile; Ag: silver).

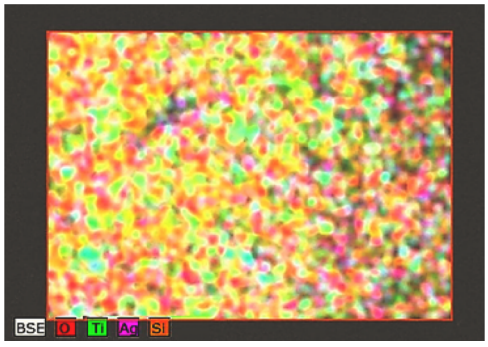

Figure 4. Electron microscopic picture of TiO_2−SiO_2−Ag film annealed at 600 °C.

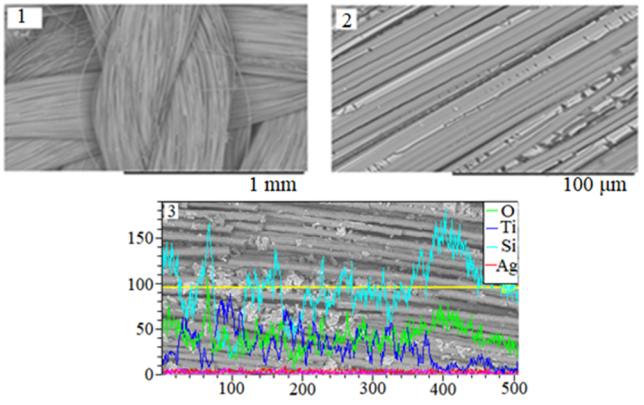

Figure 5. Morphology and surface composition for the TiO_2−SiO_2−Ag/fiberglass sample: (1) SEM image, (2) SEM image, and (3) results of elemental analysis.

The optical characteristics of TiO_2−SiO_2−Ag also have some features in comparison with TiO_2 (Table 1). The addition of additives to the system lead to a decrease in the measured values. This is probably due to the influence of silicon dioxide additives and silver particles that inhibit crystal growth processes.[20−22] The results of measurements of the gated zone width indicate the appearance of the conductivity of additives and shifted of light absorption to the visible light regime in TiO_2−SiO_2−Ag, which contains silver particles.

As a result of the contact of silver and anatase particles, there is an alignment of Fermi levels, some electrons from silver go to anatase (the silver electron yield work is 4.7 eV), and the appearance of potential barrier of 0.4 eV. In this case, one should assume the possibility of the transition of electrons through the boundary surface and to silver. As a consequence, the energy of the anatase band gap width decreased to 2.8 eV, charge separation became possible, and as a consequence, photoactivity under visible light irradiation increased.

After applying the TiO_2−SiO_2−Ag film to the surface of the fiberglass filaments, the microphotographs of TiO_2−SiO_2−Ag/fiberglass samples were obtained. The images show defects on the film surface peculiar to amorphous structures (Figure 5).

The results of the elemental analysis show that the surface of the composite fiber material TiO_2−SiO_2−Ag/fiberglass material was represented by the oxide compounds of titanium, silicon, and silver. The amorphous silicon dioxide phase in the film composition increases its adhesion[23] to the fiberglass carrier and increases the specific surface area to 12.9 m^2/g (Sd. fiberglass 0.3 m^2/g).

The high intensity of signals related to silicon is explained by the composition of the fiberglass carrier.

3.3. Antibacterial Properties of TiO_2−SiO_2−Ag/Fiberglass. The results of microbial cell CFU counts from the solutions obtained after washing the fiberglass materials used as filters showed that the use of TiO_2−SiO_2−Ag/fiberglass allows a significant reduction in the microbial cell CFU value Figure 6.

The number of microbial cells in the studied samples was 430 CFU m^{-3} for the washed fiberglass solution, which is three times higher than the content of microbial cells in the solution after washing the sample TiO_2−SiO_2−Ag/fiberglass (125 CFU m^{-3}). The result is explained by the photocatalytic destruction of microbial cells on the surface of TiO_2−SiO_2−Ag/fiberglass under the influence of light radiation. The presence of a pronounced antibacterial effect of the TiO_2−SiO_2−Ag/fiber-

Table 1. Optical Parameters of TiO_2 and TiO_2−SiO_2−Ag Samples

sample	film thickness, nm	index of refraction	energy of the bandgap, eV
TiO2 (600 °C)	34.31 ± 2.28	2.195 ± 0.007	3.2 ± 0.05
TiO_2−SiO_2−Ag (600 °C)	23.92 ± 1.24	2.154 ± 0.002	2.8 ± 0.5

https://doi.org/10.1021/acsomega.3c00969
ACS Omega 2023, 8, 23521−23527

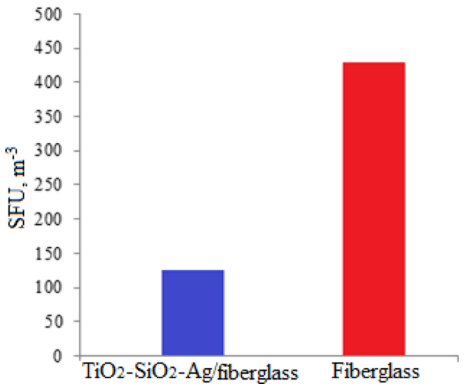

Figure 6. Results of CFU counts.

glass is also confirmed by microphotographs, as shown in Figure 7.

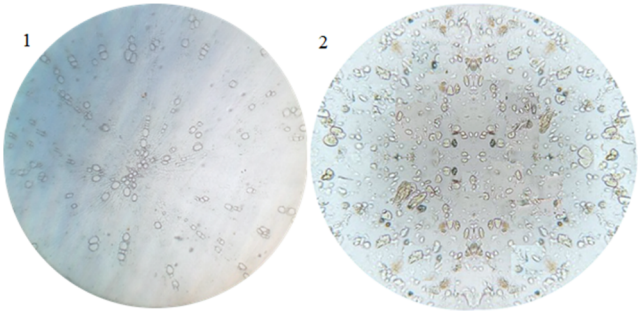

Figure 7. Micrographs of incubated bacterial cultures from solutions after washing: (1)—TiO_2−SiO_2−Ag/fiberglass, (2)—fiberglass.

The images in Figure 7 demonstrate a slower growth of microbial cells for the bacterial sample after washing with TiO_2−SiO_2−Ag/fiberglass. The group composition is characterized by the dominance of saprophytic microbial cells, which is logical since this group of microbial cells is more often found in soil and ground environments, and its distribution in air media occurs together with dust suspended solids, which tend to accumulate in closed rooms.

4. CONCLUSIONS

Microbiological air pollution is an important problem that requires the improvement of existing materials and the development of new materials. A sample of TiO_2−SiO_2−Ag/fiberglass was obtained by forming the film TiO_2−SiO_2−Ag on the surface of fiberglass filaments. The composition and concentrations of the components of the film-forming solution and the heat treatment method for the formation of TiO_2−SiO_2−Ag films on the surface of fiberglass filaments have been investigated. The influence of silicon dioxide and silver additives on phase formation on the photoactivity of titanium dioxide on the films was revealed.

The study of the antibacterial properties of the sample TiO_2−SiO_2−Ag/fiberglass showed that the use of TiO_2−SiO_2−Ag/fiberglass as a filter-sorbing material in photocatalytic air purification can reduce the number of colony-forming units of microorganisms by three times comparing with the pure fiberglass filter.

AUTHOR INFORMATION

Corresponding Author

Yu-Wen Chen − *Department of Chemical Engineering, National Central University, Jhongli 32001, Taiwan;* orcid.org/0000-0002-8519-2595; Phone: +886-34227151, ext. 34203; Email: ywchen@cc.ncu.edu.tw; Fax: +886-34252296

Authors

Aleksandr A. Buzaev − *National Research Tomsk State University, Tomsk 634050, Russia*

Ekaterina S. Lyutova − *National Research Tomsk State University, Tomsk 634050, Russia*

Valeriya A. Tkachuk − *National Research Tomsk State University, Tomsk 634050, Russia;* orcid.org/0000-0002-7784-4370

Lyudmila P. Borilo − *National Research Tomsk State University, Tomsk 634050, Russia*

Complete contact information is available at: https://pubs.acs.org/10.1021/acsomega.3c00969

Notes

The authors declare no competing financial interest.

ACKNOWLEDGMENTS

This study was supported by the Tomsk State University Development Program (Priority-2030). The work was carried out using the research equipment of the Unique Research Installation "System of Experimental Bases Located along the Latitudinal Gradient" of the National Research Tomsk State University with the financial support from the RF Ministry of Science and Higher Education (RF-2296.61321X0043, 13.UNU.21.0005, agreement no. 075-15-2021−672).

REFERENCES

(1) Piracha, A.; Chaudhary, M. T. Urban air pollution, urban heat island and human health: a review of the literature. *Sustanability* **2022**, *14*, 9234−9319.

(2) Aliabadi, A. A.; Rogak, S. N.; Bartlett, K. H.; Green, S. I. Preventing Airborne Disease Transmission: Review of Methods for Ventilation Design in Health Care Facilities. *Adv. Prev. Med.* **2011**, *2011*, 1−21.

(3) Flores, M. V.; Cohen, M. Preventing Airborne disease transmission: implication for patients during mechanical Ventilation. *Medicine* **2013**, *1*, 305−314.

(4) Pepper, I. L.; Gerba, C. P. Aeromicrobiology. *Environmental Microbiology*; Wiley Online Library, 2014; Vol. 3, pp 89−110.

(5) Naidu, R.; Biswas, B.; Willett, I. R.; Cribb, J.; Kumar Singh, B.; Paul Nathanail, C.; Coulon, F.; Semple, K. T.; Jones, K. C.; Barclay, A.; Aitken, R. J. Chemical pollution: A growing peril and potential catastrophic risk to humanity. *Environ. Int.* **2021**, *156*, 106616.

(6) Vershinin, N. N.; Balikhin, I. L.; Berestenko, V. I.; Efimov, O. N.; Kabachkov, E. N.; Kurkin, E. N. Synthesis and properties of a carbon monoxide oxidation catalyst based on plasma-chemical titanium carbonitride, titanium dioxide, and palladium. *High Energy Chem.* **2021**, *55*, 75−79.

(7) Muscetta, M.; Russo, D. Photocatalytic applications in wastewater and air treatment: a patent review. *Catalysts* **2021**, *11*, 834.

(8) Naseem, T.; Durrani, T. The role of some important metal oxide nanoparticles for wastewater and antibacterial applications: A review. *Environ. Chem. Ecotoxicol.* **2021**, *3*, 59−75.

(9) Selishchev, D.; Kozlov, D. Photocatalytic oxidation of diethyl sulfide vapor over TiO_2-Based composite photoctalysts. *Molecules* **2014**, *19*, 21424−21441.

(10) Buzaev, A. A.; Zharkova, V. V.; Kozik, V. V. *Synthesis of Stable Sols Based on TiO_2, SiO_2 and Ag^+ Ions for Thin Film Coatings with Photocatalytic Properties*; Bulletin of the University of Technology, 2021; Vol. *24*, p 5559.
(11) Ahmed, E. M. Hydrogel: Preparation, characterization, and applications: A review. *J. Adv. Res.* **2015**, *6*, 105−121.
(12) Feng, S.; Ma, D.; Qiu, Y.; Duan, L. Deep insights into the viscosity of small molecular solutions for organic light-emitting diodes. *RSC Adv.* **2018**, *8*, 4153−4161.
(13) Zhu, Y. J.; Chen, F. Microwave-assisted preparation of inorganic nanostructures in liquid phase. *Chem. Rev.* **2014**, *114*, 6462−6555.
(14) Yan, H.; Yuanhao, W.; Hongxing, Y. TEOS/silane-coupling agent composed double layers structure: a novel super-hydrophilic surface. *Energy Proc.* **2015**, *75*, 349−354.
(15) Kubiak, A.; Bielan, Z.; Bartkowiak, A.; Gabala, E.; Piasecki, A.; Zalas, M.; Zielińska-Jurek, A.; Janczarek, M.; Siwińska-Ciesielczyk, K.; Jesionowski, T. Synthesis of Titanium Dioxide via Surfactant-Assisted Microwave Method for Photocatalytic and Dye-Sensitized Solar Cells Applications. *Catalysts* **2020**, *10*, 586.
(16) Al-Madanat, O.; Curti, M.; Gunnemann, C.; Alsalka, Y.; Dillert, R.; Bahnemann, D. W. TiO_2 photocatalysis: impact of the platinum loading method on reductive and oxidative half-reactions. *Catal. Today* **2021**, *380*, 3−15.
(17) Bukhtiyarov, A. V.; Prosvirin, I. P.; Bukhtiyarov, V. XPS/STM study of model bimetallic Pd-Au/HOPG catalysts. *Appl. Surf. Sci.* **2016**, *367*, 214−221.
(18) Gaidau, C.; Petica, A.; Ignat, M.; Popescu, L. M.; Piticescu, R. M.; Tudor, I. A.; Piticescu, R. R. Preparation of silica doped titania nanoparticles with thermal stability and photocatalytic properties and their application for leather surface functionalization. *Aradian J. Chem.* **2017**, *10*, 985−1000.
(19) Selivestova, E. V.; Ibzfev, N. Kh.; Zhumabekov, A. J. Influence of cherebium nanoparticles on photodetecting properties of TiO_2/graphene oxide nanocomposites. *Opt Spectrosc.* **2020**, *128*, 13371345.
(20) Ozbay, E. Plasmonics: merging photonics and electronics at nanoscale dimensions. *Science* **2006**, *311*, 189−193.
(21) Lui, W.-L.; Lin, F. C.; Yang, Y. C.; Haung, C. H.; Huang, J. S. The influence of shell thickness of Au-TiO_2core-ahell nanoparticles on the plasmonic enhancement effect in dye-sensitized solar cell. *Nanoscale* **2013**, *5*, 7953−7963.
(22) Chemin, J. B.; Bulou, S.; Baba, K.; Fontaine, C.; Sindzingre, T.; Boscher, N. D.; Choquet, P. Transparent anti-fogging and self-cleaning TiO_2/SiO_2 thin films on polymer substrates using atmospheric plasma. *Sci. Rep.* **2018**, *8*, 9603.
(23) Bogomolova, E.; Kirtsideli, I. Airborne fungi in four stations of the St. Petersburg underground railway system. *Int. Biodeterior. Biodegrad.* **2009**, *63*, 156−160.

https://doi.org/10.1021/acsomega.3c00969
ACS Omega 2023, 8, 23521−23527